Metal–metal and ligand–ligand interactions in gold poly-yne systems†

Peiyi Li,[a] Birte Ahrens,[b] Ka-Ho Choi,[c] Muhammad S. Khan,[d] Paul R. Raithby,*[b] Paul J. Wilson[b] and Wai-Yeung Wong[c]

[a] Department of Chemistry, University of Cambridge, Cambridge, UK CB2 1EW
[b] Department of Chemistry, University of Bath, Bath, UK BA2 7AY.
 E-mail: p.r.raithby@bath.ac.uk
[c] Department of Chemistry, Hong Kong Baptist University, Waterloo Road, Kowloon Tong, Hong Kong, P. R. China
[d] Department of Chemistry, College of Science, Sultan Qaboos University, Al-Khod 123, Sultanate of Oman

Paper

The acetylide-functionalised thiophene gold(I) complexes [(PPh$_3$)Au(C≡C(C$_4$H$_2$S)(C$_4$H$_3$S))] **1**, [(PPh$_3$)Au(C≡C(C$_4$H$_2$S)C≡C)Au(PPh$_3$)] **2**, [(PR$_3$)Au(C≡C(C$_4$H$_2$S)$_2$C≡C)Au(PR$_3$)] (R = Ph **3**, Cy **4**) and [(PPh$_3$)Au(C≡C(C$_4$H$_2$S)$_3$C≡C)Au(PPh$_3$)] **5** have been prepared by the reaction of the trimethylsilylethynyl oligothiophene with KOH/MeOH, followed by the addition of a stoichiometric amount of the gold(I) phosphine chloride and NaOMe in MeOH. The products have been characterised spectroscopically and their single crystal X-ray structures determined. In the molecular structures of all the complexes the Au(I) centres adopt the expected linear, two-coordinate geometry, except that in **2** the material forms a polymer through additional Au⋯Au interactions [Au⋯Au 3.2915(10) and 3.2347(9) Å] between the molecular units. With the longer acetylene-functionalised spacer groups no Au⋯Au interactions are present, but hydrogen bonding and π⋯π interactions are of significance. The solution absorption and emission spectra of these complexes have been recorded and the maxima are increasingly red-shifted as the length and planarity of the functionalised spacer groups increases which is consistent with the absorptions and emissions being dominated by ligand-centred π–π* transitions.

Introduction

Recent interest in gold(I) σ-acetylide complexes and in related polymers has been stimulated by the observation that many of these materials are luminescent,[1–3] in addition to the possibility that they may exhibit novel electrical conducting and nonlinear optical behaviour.[4]

The initial studies that confirmed that gold(I) σ-acetylides represented a new class of luminophores were carried out on the dinuclear complex [Au$_2$(μ-dppe)(C≡CPh)$_2$].[5] An X-ray crystal structure of this complex established that there was an intermolecular Au⋯Au interaction of 3.152(2) Å that holds two complexes together in a transoid configuration to form a dimer. The molecule exhibited a strong solid-state emission that originates from a $(d_{\delta*})^1(p_\sigma)^1$ triplet excited state, where the $d_{\delta*}$ antibonding state results from interactions between the two $5d_{xy}$ and the two $5d_{x^2-y^2}$ orbitals from the two gold centres, and the p_σ state originates from the interactions between the two 6p orbitals. Clearly, the presence of the Au⋯Au interaction is key to the luminescent properties of the compound.

Following the first example of luminescent gold(I) σ-acetylides a plethora of studies have been undertaken. Key results that help to elucidate the factors that influence the luminescent properties of these materials include the discovery of a non-covalently bonded polymer[1] that forms in the solid state *via* intermolecular Au⋯Au interactions in [Au$_2$(μ-(PPh$_2$-2-py-6-PPh$_2$))(C≡C–Ph)$_2$] [Au⋯Au distance: 3.252(1) Å]. The solid state material emits at 500 nm. This is at higher energy than [Au$_2$(μ-dppe)(C≡C–Ph)$_2$], and Che and coworkers[5] ascribed this difference to a shorter Au⋯Au distance in [Au$_2$(μ-dppe)-(C≡C–Ph)$_2$], assuming the origin of this emission is also from a $(d_{\delta*})^1(p_\sigma)^1$ triplet excited state. Yam *et al.* have synthesised a series of gold(I) σ-acetylides [(P(*p*-Tol)$_3$)Au–(BL)–Au(P-(*p*-Tol)$_3$))] (BL = 1,4-diethynylbenzene and 9,10-diethynylanthracene), [Au$_2$(μ-P^P)(C≡C–R)$_2$] {P^P = dppn [dppn = 1,8-bis(diphenylphosphino)naphthalene], R = C$_6$H$_4$-Ph-4, C$_6$H$_4$-OCH$_3$-4, n-C$_6$H$_{13}$; P^P = dcpn [dcpn = 1,8-bis(dicyclohexylphosphino)naphthalene], R = C$_6$H$_4$-Ph-4; P^P = dmpm [dmpm = bis(diphenylphosphino)methane], R = Ph, C$_6$H$_4$-OCH$_3$-4} and [Au$_3$(μ$_3$-dmmp)(C≡C–R)$_3$] [R = Ph, C$_6$H$_4$-OCH$_3$-4; dmmp = bis(dimethylphosphinomethyl)methylphosphine].[6] These alkynylgold(I) phosphine complexes exhibit rich luminescent behaviour with long-lived excited states. The origin of the emission is strongly dependent on the nature of the phosphine ligands and the acetylide units. All of the complexes are strong reducing agents in the excited states, capable of undergoing facile electron transfer reactions with pyridinium acceptors. A related series of dinuclear and tetranuclear gold(I) σ-acetylides, [Au$_2$(μ-dppb)(C≡C–R)$_2$] [dppb = 1,4-bis(diphenylphosphino)benzene; R = n-C$_6$H$_{13}$, Ph, C$_6$H$_4$-OCH$_3$-4] and [Au$_4$(μ$_4$-tppb)(C≡C–R)$_4$] [tppb = 1,2,4,5-tetrakis-(diphenylphosphino)benzene; R = n-C$_6$H$_{13}$, Ph, C$_6$H$_4$-OCH$_3$-4], have been prepared.[7] Again, Au⋯Au interactions are observed in the tetranuclear complexes, although in this case they are intramolecular. All complexes are emissive and the emission states are assigned to be either intraligand π–π* or σ(Au–P)–π*. Recently, Puddephatt and co-workers have presented a series of gold(I) σ-acetylides with the formulae [(PMe$_3$)-Au(C≡C–Ar–C≡C)Au(PMe$_3$)] (Ar = C$_6$H$_4$, 2,5-Me$_2$C$_6$H$_2$),[8]

[3,5-Me$_2$C$_6$H$_3$–(C≡CAuL)$_2$] [L = P(OPh)$_3$, P(OMe)$_3$, PPh$_3$, PMePh$_2$][9] and [C$_6$H$_4$(OCH$_2$C≡CAu)$_2${μ-Ph$_2$P(CH$_2$)$_n$PPh$_2$}] (n = 1–6).[10] The solid-state structure of [(PMe$_3$)Au(C≡C-2,5-Me$_2$C$_6$H$_2$–C≡C)Au(PMe$_3$)] shows intermolecular Au···Au interactions which lead to a zigzag chain polymer. The complexes [(PMe$_3$)Au(C≡C–Ar–C≡C)Au(PMe$_3$)] are luminescent in solution, and the emission is derived from ^{3}(π–π*) or ^{3}(σ–π*) excited states associated with the Au–C≡CPh group. A significant red shift of the emission is observed in the solid state, signalling the involvement of a metal-centred ^{3}[(d$_{δ*}$)^1(p$_σ$)^1] excited state as a result of intermolecular Au···Au interactions. Similarly, the [3,5-Me$_2$C$_6$H$_3$–(C≡CAuL)$_2$] complexes exist in the solid state as infinite one-dimensional ribbon structures in which neighbouring molecules are linked through weak Au···Au interactions. They also emit in both solution and the solid state. Again, the solution emission arises from a ^{3}[σ(AuC)–π*] excited state, while the red-shifted, solid-state emission is related to the intermolecular Au···Au interactions.

From the solid state structures of gold(I) σ-acetylides reported so far, a study of the L–Au–C≡CR (L = phosphine, R = aryl group) fragments shows that Au–L, Au–C and C≡C bond lengths vary in a narrow range irrespective of the significant changes in L and R. The molecular shape seems mostly determined by the aryl group(s) in the acetylide ligand. However, in the solid state the complementary intermolecular forces of Au···Au interactions, hydrogen bonding, π–π stacking and other non-covalent interactions combine to produce novel dimers, oligomers, chains and two-dimensional networks. In many cases, it is the combination of these interactions that determines the solid-state luminescent properties of these materials.

Our interest in gold–acetylide polymers and their molecular precursors stems from our related studies on opto-electronically active platinum poly-yne complexes and polymers where conjugation along the rigid molecular backbone is responsible for their luminescent properties.[11] In particular, studies on acetylide-functionalised oligothiophene platinum(II) complexes and polymers have shown that as the number of thiophene rings in the system increases the optical band gap is reduced, but that intersystem crossing from the singlet excited state to the triplet excited state is also reduced.[12,13] We now report the extension of our studies to include a series of gold(I) complexes with the four acetylide-functionalised thiophenes shown in Fig. 1, and discuss the nature of the intermolecular interactions observed in their crystal structures, and their luminescent properties in solution.

Results and discussion

Synthesis and spectroscopic characterisation

The trimethylsilyl-protected ligands, (TMS)$_2$L$^{2–4}$, can easily be proto-desilylated by reaction with methanolic KOH to afford the terminal acetylide-functionalised thiophenes, H$_2$L$^{2–4}$. The trimethylsilyl-protected ligand, (TMS)L^1, is obtained by the coupling of 5-bromo-2,2′-bithiophene[14] with trimethylsilylacetylene using the well-established palladium coupling method.[15]
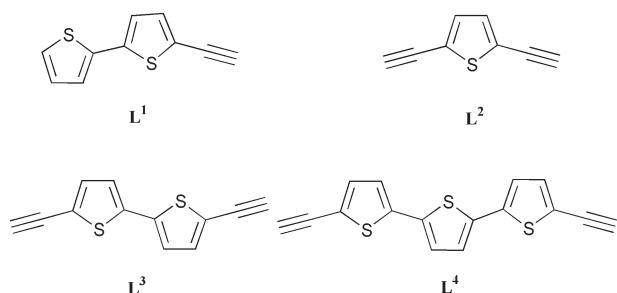
This ligand can then be proto-desilylated to give HL^1 using methanolic KOH. The terminal acetylenes are not stable in solution or on exposure to light for long periods, so the freshly prepared alkyne is best treated immediately with a stoichiometric quantity of the gold phosphine chloride, in CH$_2$Cl$_2$, followed by NaOMe in MeOH. The reaction is complete after stirring at room temperature for 16 h under a dinitrogen atmosphere. Yellow crystalline products are obtained in good yields after purification by column chromatography, and recrystallisation from CH$_2$Cl$_2$–hexane. The complexes are stable in the absence of light or heat, and are soluble in chlorinated solvents but only slightly soluble in tetrahydrofuran or toluene.

All the mono- and di-nuclear gold(I) σ-acetylides have been characterised by IR and NMR spectroscopy, mass spectrometry, and microanalysis. A single characteristic v(C≡C) band is observed in all IR spectra and confirms the linear arrangement in the digold systems.[12] The ^{1}H and ^{13}C NMR spectra of the dinuclear gold(I) σ-acetylides 2–5 display similar features to those of mononuclear gold(I) σ-acetylide 1. Compared to the trimethylsilyl-protected alkyne ligands, the ^{1}H and ^{13}C NMR spectra of gold(I) σ-acetylides change little upon coordination to the gold–phosphine fragment, indicating that the interaction between Au(I) and the acetylide ligand is not significantly different from that with the trimethylsilyl group. All the dinuclear gold(I) σ-acetylides display a singlet in their ^{31}P{^{1}H} NMR spectra, consistent with the presence of equivalent phosphorus, and thus gold centres. While a molecular ion peak [M]$^+$ or [MH]$^+$ is present in the mass spectra of the mono- and di-nuclear gold(I) σ-acetylides, the most intense peak is at m/z 459 or 477, attributable to [Au(PPh$_3$)]$^+$ or [Au(PCy$_3$)]$^+$.

Molecular and crystal structures

The molecular structure of [(PPh$_3$)Au(C≡C(C$_4$H$_2$S)(C$_4$H$_3$S))] 1 is shown in Fig. 2 and selected bond parameters are listed in Table 1. The molecule adopts the expected rod-like geometry with the two-coordinate Au(I) centre adopting a near linear geometry. The Au–C(≡C) and Au–P bond lengths are within the range found in previously reported phosphine-substituted gold σ-acetylides.[5–10,16] However, the Au–P distance is longer than in [Au(PPh$_3$)Cl],[17] due to the stronger trans influence of the acetylide compared with the chloride ligand. The C≡C bond length and the bond parameters within the two thiophene rings are also within the expected range.[12] However, the dihedral angle between the two adjacent thiophene rings is 43.6°, which is in marked contrast to the conformation in the related dinuclear platinum complex [(Ph)(PEt$_3$)$_2$Pt(C≡C-(C$_4$H$_2$S)(C$_4$H$_2$S)C≡C)Pt(PEt$_3$)$_2$(Ph)] and in its precursor [Me$_3$Si-(C≡C(C$_4$H$_2$S)$_2$C≡C)SiMe$_3$] where the two thiophene rings lie in the same plane.[12]

An inspection of the crystal packing diagram of 1 (Fig. 3) readily explains the large dihedral angle between the two thiophene rings in the functionalised acetylene ligand. The terminal thiophene twists to accommodate a weak intermolecular, electrostatic interaction of the sulfur atom in this ring
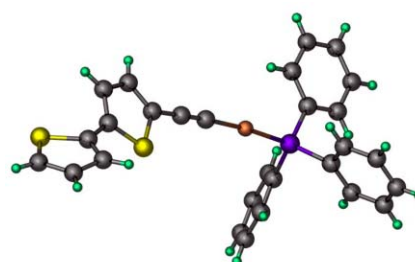

Fig. 1 The four acetylide-functionalised thiophenes.

L^1 L^2 L^3 L^4

Fig. 2 Molecular structure of [(PPh$_3$)Au(C≡C(C$_4$H$_2$S)(C$_4$H$_3$S))] 1.

Table 1 Selected bond lengths (Å) and angles (°) for the gold complexes **1**–**5**

|	[Au]–C(≡C)	[Au]–P	C≡C	(C≡)C–[Au]–P	C≡C–[Au]
1	2.000(4)	2.2815(11)	1.202(6)	175.5(2)	177.1(5)
2[a,b]	1.997(6)	2.2787(17)	1.201(8)	165.86(17)	166.1(5)
	2.005(6)	2.2780(18)	1.187(8)	166.00(18)	167.8(6)
3	2.004(4)	2.2747(11)	1.194(6)	177.50(11)	177.4(4)
4[c]	1.995(4)	2.2901(12)	1.195(6)	178.71(15)	176.6(5)
5[d]	2.003(10)	2.277(3)	1.197(14)	174.0(3)	167.6(11)
	2.004(10)	2.274(3)	1.219(15)	174.9(3)	169.6(11)

[a] Two independent molecules in the asymmetric unit. [b] Au···Au separation 3.2915(10) and 3.2347(9) Å. [c] [Au] = Au(PCy₃). [d] Two independent [Au] units.
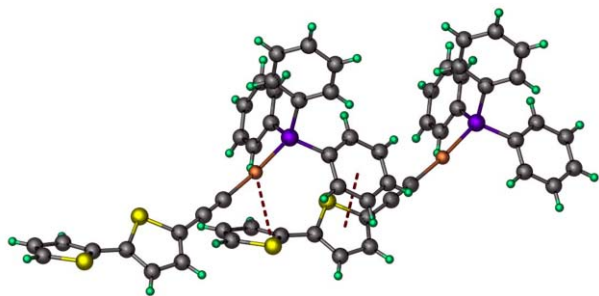
Fig. 3 Packing diagram for [(PPh₃)Au(C≡C(C₄H₂S)(C₄H₃S))] **1** showing the Au···S and π···π interactions. Click image or here to access a 3D representation.

with a gold centre in an adjacent molecule, with an interaction distance of 3.841 Å. The best evidence for this weak interaction comes from the twisting of the thiophene ring as there is little distortion of the linear geometry at the gold centre. A possible explanation for this interaction involves the donation of electron density from a lone pair on the sulfur atom to an empty hybrid orbital on the gold. The other significant intermolecular interaction involves a π···π interaction between the inner thiophene ring of one molecule with one of the phenyl rings of the triphenylphosphine group on an adjacent molecule. The centroid···centroid distance between these rings is 3.817 Å, and the interplanar angle is 12.9°.

What is perhaps more significant about the structure of **1** is the absence of weak intermolecular Au···Au interactions that have been observed in the solid state structures of many gold(I) acetylide and related complexes.[1–3] These 'aurophilic' d¹⁰···d¹⁰, non-covalent Au···Au interactions have strengths comparable to those of hydrogen bonds, and may arise from the correlation effects that are enhanced by relativistic effects.[18,19] The closest comparable complex with **1** is [(PPh₃)Au(C≡CPh], which exhibits weak intermolecular Au···Au interactions [3.379(1) Å] linking two [(PPh₃)Au(C≡CPh] molecules together in a nearly orthogonal arrangement to give a loosely bonded dimer.[20] Since the local environment around the gold centres in each complex is similar it is surprising that there are no Au···Au short contacts in **1**. However, the lack of sulfur functionality in [(PPh₃)Au(C≡CPh)] precludes the opportunity for Au···S interactions.

The situation is somewhat different in the digold complex [(PPh₃)Au(C≡C–(C₄H₂S)–C≡C)Au(PPh₃)] **2** where intermolecular Au···Au interactions [3.2915(10) and 3.2347(9) Å] link the molecular units together, as shown in Fig. 4, to form a loose polymer. Selected bond parameters are listed in Table 1. The asymmetric unit contains two molecular units, and the Au···Au interactive {(Ph₃P)AuC≡C–} vector is anti-parallel with a torsion angle (–C≡C–Au···Au–C≡C–) of 172.2°. If the Au···Au interactions are ignored, each gold centre is two-coordinate, but the (C≡)C–Au–P angles show a *ca.* 14° deviation from linearity that is greater than normally observed in gold acetylide complexes that do not involve Au···Au interactions. The observed deviation in this case can be
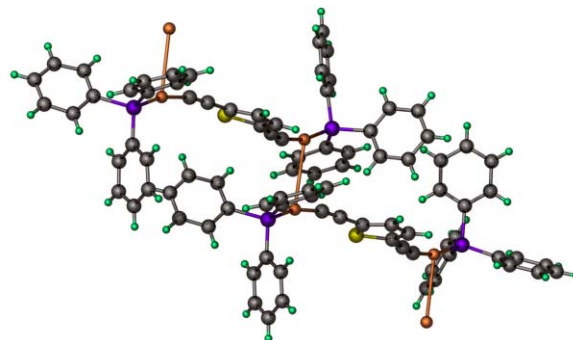
Fig. 4 Structure of the [(PPh₃)Au(C≡C–(C₄H₂S)–C≡C)Au(PPh₃)]∞ **2** polymer showing the Au···Au interaction. The triphenylphosphine groups are positionally disordered and only one orientation of the rings is shown for clarity. Click image or here to access a 3D representation.

attributed to the d¹⁰···d¹⁰ interactions as the distortion is consistent with pairs of gold centres being drawn closer together. The dimensions of the (–C≡C–(C₄H₂S)–C≡C–) unit are comparable with those observed in [(Ph)(PEt₃)₂Pt-(C≡C(C₄H₂S)C≡C)Pt(PEt₃)₂(Ph)].[12] The Au–P distances are similar to the value of 2.2815(11) Å found in **1**.

Despite the presence of the sulfur atom in the single ring linker group there are no short Au···S interactions, and in **2** the Au···Au interactions dominate. The presence of Au···Au interactions where there is a single aromatic ring between the acetylenic groups has also been observed in [(P(MeO)₃)Au(C≡C–(3,5-Me₂C₆H₂)–C≡C)Au(P(OMe)₃)], [(PMePh₂)Au(C≡C–(3,5-Me₂C₆H₂)–C≡C)Au(PMePh₂)][9] and [(PMe₃)Au(C≡C–p-C₆H₄–C≡C)Au(PMe₃)].[8] In each of these examples there are no functionalities associated with the central ring that could become involved in strong intermolecular interactions although C–H···Au interactions are possible. What is notable in this series is that the Au···Au distance in [(PMe₃)Au(C≡C–p-(C₆H₄)–C≡C)Au(PMe₃)],[8] at 3.1361(9) Å, is shorter than the interaction distance in the other complexes, and this may be related to the fact that PMe₃ is less bulky than each of PPh₃, P(OMe)₃ and PMe₂Ph.

In the complexes [(PPh₃)Au(C≡C–(C₄H₂S)₂–C≡C)Au(PPh₃)] **3** and [(PCy₃)Au(C≡C–(C₄H₂S)₂–C≡C)Au(PCy₃)] **4** the length of the central spacer group has been extended by one thiophene ring compared with **2**. The molecular structures of **3** and **4** are shown in Figs. 5 and 6, respectively, and selected bond parameters are presented in Table 1. Unlike **2**, the complexes **3** and **4** exist within the crystal as discrete molecular units. They are not isomorphous, and **3** crystallises with a solvent molecule of CH₂Cl₂ in the lattice, and the digold species sits on a crystallographic centre of symmetry at the mid-point of the central C–C bond. Similarly, **4** crystallises with one digold complex and one CH₂Cl₂ molecule in the asymmetric unit.

The gold centres in **3** and **4** are purely two-coordinate, and consequently the (C≡)C–Au–P and C≡C–Au angles show little deviation from linearity, in contrast with those of **2**. The Au–C(≡C) and C≡C bond lengths are also similar in both compounds, and are also similar to those found in complexes **1**
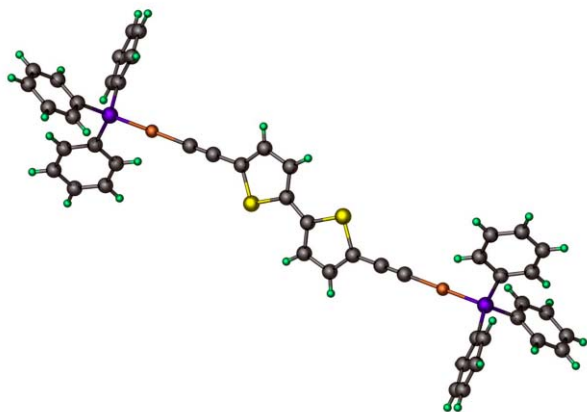
Fig. 5 Molecular structure of $[(PPh_3)Au(C≡C–(C_4H_2S)_2–C≡C)Au(PPh_3)]$ **3**. The molecule sits on a crystallographic centre of symmetry.
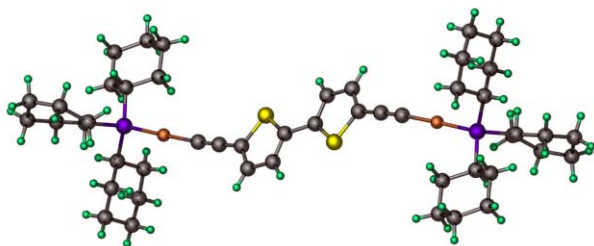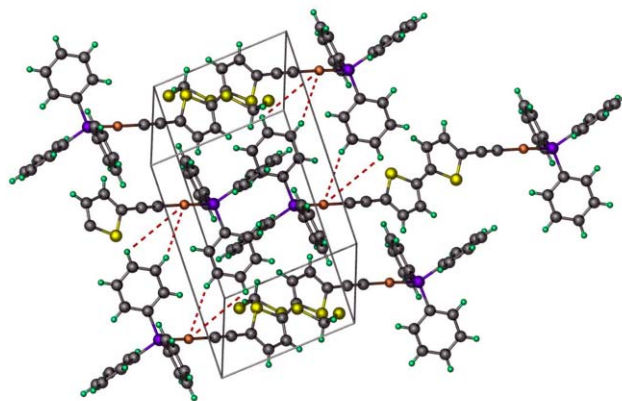

Fig. 6 Molecular structure of $[(PCy_3)Au(C≡C–(C_4H_2S)_2–C≡C)Au-(PCy_3)]$ **4**. One of the phosphine ligands and one of the thiophene rings suffer from positional disorder, and only one orientation of each is shown for clarity.

and **2**. However, the Au–P distance in **4** is *ca.* 0.15 Å longer than that in either **2** or **3**. This is consistent with the presence of the PCy_3 group in **4** which has considerably greater steric bulk than PPh_3, and is also a poorer π-acceptor. As noted from the similarity of the C≡C distances, this difference is not transmitted to the acetylide ligand by the Au(I) centre. This is probably due to the low energy σ(Au–P) obital being buried well below the σ(Au–C) and π orbitals of the acetylide ligand. This insensitivity of the coordinated acetylene ligand towards the ancillary ligand around the gold is also manifested in their absorption and emission spectra (*vide infra*).

Within the central dithiophene group of **3** and **4** the two rings exhibit the expected *anti* configuration as this minimises the repulsion between the β-hydrogens on the adjacent rings. In the case of **3** the two rings are precisely planar by crystallographic symmetry, as in the related diplatinum complex $[(Ph)(PEt_3)_2Pt(C≡C(C_4H_2S)(C_4H_2S)C≡C)Pt(PEt_3)_2(Ph)]$,[12] whereas in **4** one of the rings shows positional disorder and an accurate assessment of the dihedral angle is not possible, although the average arrangement is close to planar. This contrasts to the situation in **1** where the two adjacent rings are twisted by 43.6° to accommodate the Au···S intermolecular interactions.

In **3** and **4** there are no Au···Au or Au···S short contacts, and the closest intermolecular interactions involve the dichloromethane molecule and one of the acetylenic C–C bonds, with C–H···C(≡C) and C–H···(C≡)C distances of 2.811 and 2.951 Å. There are also contacts between the gold centres and aromatic hydrogens from a phenyl ring on the phosphine groups of an adjacent molecule of 3.236 Å and above. A packing diagram for **3** is shown in Fig. 7. It appears that with a longer spacer group between the gold centres the Au···Au intermolecular interactions that dominate for the digold systems with a shorter spacer group are no longer favoured, and in the case of **3** and **4** Au···S interactions are not of significance either.

Fig. 7 Crystal packing diagram for $[(PPh_3)Au(C≡C–(C_4H_2S)_2–C≡C)Au(PPh_3)]$ **3** showing the shortest intermolecular contacts. Click image or here to access a 3D representation.

In order to test this hypothesis further, the structure of the digold complex with the acetylene-functionalised terthiophene ligand was determined. The molecular structure of $[(PPh_3)Au(C≡C–(C_4H_2S)_3–C≡C)Au(PPh_3)]$ **5** is shown in Fig. 8 and selected bond parameters are listed in Table 1. Again, the molecule adopts a rod-like structure with the bond parameters involving the gold, the phosphorus and the acetylene unit being very similar to those in **3**. The terthiophene groups adopt the expected planar, *anti* configuration with dihedral angles between the central and the outer rings of 8.70 and 5.04°, respectively.

The molecule crystallises in the triclinic space group $P\bar{1}$ with one molecule in the asymmetric unit. The crystal packing diagram shown in Fig. 9 illustrates the absence of Au···Au short contacts, which is consistent with the near linearity of the P–Au–C(≡C) unit. Nor are there any significant Au···S contacts, and the shortest intermolecular interactions involve a hydrogen from a phosphine phenyl ring on one molecule interacting with the C≡C bond in an adjacent molecule, C–H···C, each of 2.817 Å.

On this structural evidence, it does seem to be the case that as the linker group between the gold centres in acetylene-functionalised complexes becomes longer the possibility of oligomer or polymer formation through non-covalent intermolecular interactions significantly decreases.

Electronic and emission spectroscopy

Absorption and emission spectral data, recorded at room temperature in CH_2Cl_2 solution using a concentration of
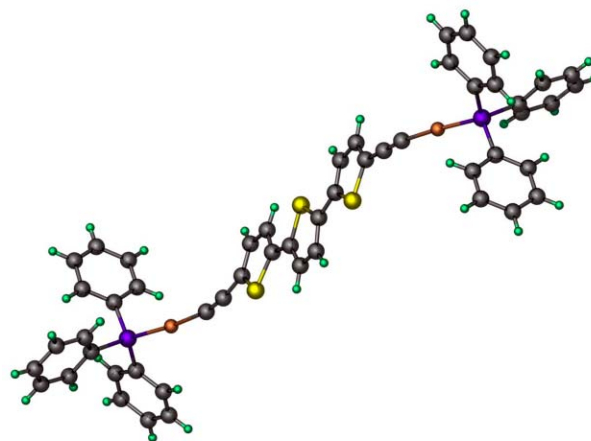
Fig. 8 Molecular structure of $[(PPh_3)Au(C≡C–(C_4H_2S)_3–C≡C)Au-(PPh_3)]$ **5**.
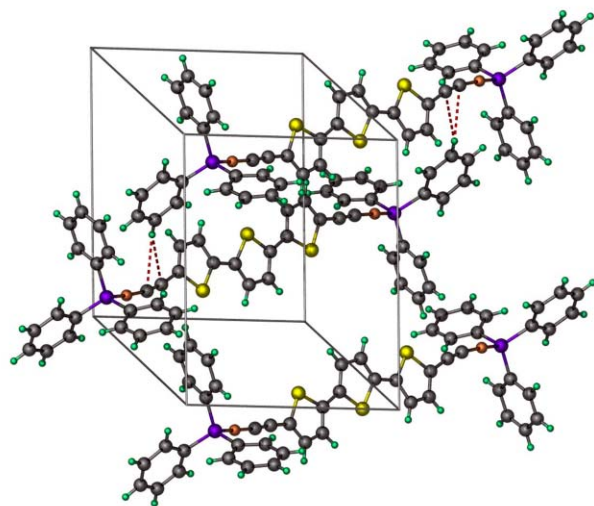
Fig. 9 Crystal packing diagram for [(PPh₃)Au(C≡C–(C₄H₂S)₃–C≡C)-Au(PPh₃)] **5** showing the shortest intermolecular contacts. Click image or here to access a 3D representation.

10^{-5} mol dm^{-3} for complexes **1**–**5** and for the terminal acetylene compounds **HL**^{1} and **H₂L**$^{2-4}$ (prepared by the treatment of the trimethylsilyl-protected acetylenes with KOH–MeOH) to provide a comparison, are listed in Table 2.

In general, the gold(I) complexes **1**–**5** absorb strongly in the range 290–450 nm, and the peak shape of the complex is similar to that of its parent acetylide ligand, but the peak maxima are shifted to longer wavelength. The strong dependence of the absorption spectra on the nature of the acetylide ligands suggests that transitions are π–π* ligand-centred and the insensitivity of the low energy absorption bands towards the ancillary ligands on the gold centre (*cf.* **3** *vs.* **4**) precludes an Au(I)-centred origin for these transitions. However, the red shift of the spectra in the complexes indicates π-interaction of the gold centres with the acetylide bridges. Therefore, the spectra are likely to be dominated by ligand π–π* transitions, but mixed with a small contribution from σ(Au–C) in the HOMO and some Au 6p$_\pi$ in the LUMO.[8] Although the possibility of an MLCT origin for these absorptions cannot be ruled out totally, it must be of minor importance, since the absorption and emission spectra for **2** in the less polar solvent, toluene (absorption: λ$_{max}$ 342, 366 nm; emission: λ 378, 394 nm), showed insignificant differences from those in CH₂Cl₂. However, it should be noted that the spectra were measured in solution where Au(I)···Au(I) inter-actions are likely to be less significant, particularly for **2**.

The increase in λ$_{max}$ (Δλ$_{max}$: 21 nm for **1** *vs.* **HL**^{1}) upon introducing one Au(PPh₃) unit onto a mono-acetylene ligand, is approximately half the value after the introduction of two Au(PPh₃) units onto the corresponding diacetylene ligand (Δλ$_{max}$: 36 nm for **3** *vs.* **HL**^{3}). Similarly, the change in the absorbance maxima is also roughly half the value. As the

number of bridging aromatic rings increases there is a sequential increase in the absorption maxima; however, the value of the red shift associated with the coordination of the gold-containing fragment decreases, *i.e.* in going from **2** to **3** to **5**. This is consistent with the gold-centred orbitals contributing less to the HOMO and LUMO levels as the number of rings increases, and hence π-conjugation increases.

The complexes **1**–**5** show emission maxima that follow the same trend as their absorption maxima. There is little change in the emission spectra upon variation in the excitation wave-length indicating that a single emissive state or multiple states in equilibrium is/are responsible for the observed emission. The emission maxima are dependent on the nature of the acetylide ligand and thus the lowest emissive states in the complexes can tentatively be assigned as gold-perturbed ¹(π–π*) transitions. The relative intensity of the higher energy peak in the emission spectrum of complexes **2**, **3** and **5** increases in moving from the monothiophene to the terthiophene. The average change per bond from the geometric relaxation upon excitation diminishes as the number of linking rings increases, which leads to the higher intensity of a transition to the lower vibronic states, according to the Franck–Condon principle.[21]

Conclusions

A series of mono- and di-gold acetylene-functionalised thiophene complexes have been synthesised. An investigation of their solid state structures using X-ray crystallography shows that for the digold system with one thiophene group [(PPh₃)Au(C≡C–(C₄H₂S)–C≡C)Au(PPh₃)] **2** a loose polymeric structure is formed through 'aurophilic' Au···Au interactions. However, for the mono-gold complex [(PPh₃)Au(C≡C(C₄H₂S)-(C₄H₃S))] **1** intermolecular Au···S and π···π interactions are dominant, and for the complexes [(PPh₃)Au(C≡C–(C₄H₂S)₂–C≡C)Au(PPh₃)] **3**, [(PCy₃)Au(C≡C–(C₄H₂S)₂–C≡C)Au(PCy₃)] **4** and [(PPh₃)Au (C≡C–(C₄H₂S)₃–C≡C)Au(PPh₃)] **5** neither Au···Au nor Au···S intermolecular interactions are observed. Thus the formation of polymeric gold acetylide systems through Au···Au interactions is highly dependent on the length and steric properties of the acetylene-functionalised spacer group, and is seemingly restricted to complexes with only one ring between the two acetylenic units in the digold systems. By comparison, the related platinum complexes [PhPt(PEt₃)₂(C≡C–(C₄H₂S)$_n$–C≡C)Pt(PEt₃)₂Ph] (n = 1–3)[12,13] do not show any significant intermolecular interactions, regardless of the value of n. This probably reflects the increase in steric shielding around the core of the molecule caused by the presence of two bulky phosphine groups around each square planar platinum(II) centre.

The solution absorption and emission spectra of the complexes **1**–**5** are dominated by ligand-centred π–π* transi-tions, but are mixed with a small contribution from σ(Au–C) in the HOMO and some Au 6p$_\pi$ in the LUMO, which is consistent with the peak shape of the complex being similar to that of its parent acetylide ligand, but with the peak position shifted to

Table 2 Absorption and emission data for ligands **HL**^{1} and **H₂L**$^{2-4}$ and for complexes **1**–**5** in CH₂Cl₂ at 20 °C

	Absorption, λ/nm (ε/10⁴ M^{-1} cm^{-1})	Emission,^{a} λ/nm (relative intensity^b)
HL^1	333 (*ca.* 2.2)	392 (1)
H₂L^2	293 (*ca.* 3.8), 297 (*ca.* 3.7), 305 (*ca.* 3.2)	—
H₂L^3	341 (sh, *ca.* 2.3), 355 (*ca.* 2.5), 381 (sh, *ca.*1.2)	393 (sh, 0.83), 412 (1)
H₂L^4	394 (*ca.* 3.1)	446 (0.91), 469 (1)
1	354 (3.2), 380 (sh, 1.7)	393 (0.88), 411 (1)
2	339 (6.0), 361 (6.9)	374 (0.86), 390 (1)
3	373 (sh, *ca.* 4.8), 391 (*ca.* 5.4), 415 (sh, *ca.* 3.6)	432 (1), 455 (0.98), 495 (sh, 0.34)
4	370 (sh, 4.2), 390 (5.0), 414 (sh, 3.3)	430 (1), 453 (0.95), 495 (sh, 0.33)
5	401 (sh, 5.5), 421 (6.0), 451 (sh, 3.5)	472 (1), 499 (0.80), 545 (sh, 0.26)

^{a}Excited at λ$_{max}$. ^{b}Intensity of the strongest peak is assigned as unity.

longer wavelength. The peak maxima are increasingly red-shifted as the length and planarity of the functionalised spacer groups increase. Overall, the evidence suggests that there is little communication between the gold centres in these molecules. However, the data are from solution, and the magnitude of $Au(I)\cdots Au(I)$ interactions may be different to those in the solid state, particularly for **2**.

Experimental

General

All reactions were carried out under an atmosphere of dry dinitrogen using standard Schlenk techniques. Solvents were freshly distilled, dried and degassed before use by standard procedures.[22] Infrared spectra were recorded as solutions in a NaCl cell using a Perkin Elmer Paragon 1000 FT-IR spectrometer. UV/vis spectra were recorded using either a Perkin-Elmer Lamda-12 or a Cary 100 Bio UV-visible spectrometer. ^{1}H, ^{13}C\{^{1}H\} and ^{31}P NMR spectra were recorded using a either a Bruker DRX-400 or a Bruker DRX-500 spectrometer. Chemical shifts in ppm are referenced relative to residual solvent resonances (^{1}H and ^{13}C) and external 85% H_3PO_4 (^{31}P). Mass spectra were recorded using Kratos Concept/MSI Concept IH/Micromass Platform-LC mass spectrometers. Elemental analyses were performed at the Department of Chemistry, University of Cambridge. Solution emission spectra were recorded at 293 K using an AMINCO Bowman Series 2 Luminescence Spectrometer as 10^{-5} mol dm^{-3} solutions in CH_2Cl_2.

The starting material [Au(PPh$_3$)Cl] was prepared by a literature method,[23] whereas [Au(PCy$_3$)Cl] was prepared by the reaction of [Au(tht)Cl] with PCy$_3$.[24] The organic precursors 2,5-bis(trimethylsilylethynyl)thiophene (**L^2**), 5,5′-bis(trimethylsilylethynyl)-2,2′-bithiophene (**L^3**) and 5,5″-bis(trimethylsilylethynyl)-2,2′:5′,2″-terthiophene (**L^4**) were prepared as described previously.[12]

Ligand synthesis

5-(Trimethylsilylethynyl)-2,2′-bithiophene (TMSL^1). To 5-bromo-2,2′-bithiophene (1.48 g, 6.0 mmol) in THF (*ca.* 50–100 mL) and ^{i}Pr$_2$NH (*ca.* 50–80 mL) were added Pd(OAc)$_2$ (1 mol%), CuI (2 mol%) and PPh$_3$ (5 mol%) under N$_2$. After the mixture was stirred at room temperature for *ca.* 15–20 min, trimethylsilylacetylene (20 mol% excess) was added. The mixture was stirred for a further 15–20 min at room temperature before it was refluxed for *ca.* 15–24 h under N$_2$. The completion of the reaction was confirmed by IR and TLC. The reaction mixture was filtered and the filtrate evaporated to dryness on a rotary evaporator. The residue was dissolved in dichloromethane and washed successively with 10% HCl, water, saturated NaHCO$_3$ and water. The dichloromethane solution was dried over MgSO$_4$ and evaporated to dryness on a rotary evaporator. The crude product was purified by silica column chromatography with pentane. Yield: 0.9 g (57%), light yellow powder. IR (CH$_2$Cl$_2$): v(C≡C) 2142 cm^{-1}. ^{1}H NMR (400 MHz, CDCl$_3$): δ 0.24 (s, 9H, TMS), 6.99 (d, $^3J_{HH}$ = 3.8Hz, 1H, H^4), 7.00 (dd, $^3J_{HH}$ = 5.1 Hz, $^3J_{HH}$ = 3.6 Hz, 1H, H$^{4'}$), 7.11 (d, $^3J_{HH}$ = 3.8 Hz, 1H, H^3), 7.16 (dd, $^3J_{HH}$ = 3.6 Hz, $^4J_{HH}$ = 1.1 Hz, 1H, H$^{3'}$), 7.12 (dd, $^3J_{HH}$ = 5.1 Hz, $^4J_{HH}$ = 1.1 Hz, 1H, H$^{5'}$). ^{13}C NMR (400 MHz, CDCl$_3$): δ −0.21 (C of TMS); 97.34, 99.87 (–C≡C–); 121.77 (ipso-C), 123.21, 124.21, 124.97, 127.87, 133.37, 136.65 (ipso-C), 138.83 (ipso-C) (aromatic C of thiophenes). LSIMS (m/z): 263 (calc. M_r = 262.461). Anal. calc. for C$_{13}$H$_{14}$S$_2$Si: C, 59.49; H, 5.38. Found: C, 59.59; H, 5.41%.

Complex synthesis

General synthetic procedure for preparing the Au(I) complexes. To the freshly prepared terminal alkyne (*ca.* 0.2 mmol, from the reaction of thetrimethylsilyl-protected alkyne with KOH/MeOH) in CH$_2$Cl$_2$ (30 mL) was added gold(I) phosphine chloride (stoichiometric amount), followed by MeOH/NaOMe (20 mL, containing *ca.* 20–30 mg Na). The mixture was stirred under N$_2$ at room temperature overnight and then filtered through cellulose. The filtrate was evaporated to dryness under reduced pressure. CH$_2$Cl$_2$ was added to the residue and the resulting suspension was stirred for 15 min and filtered. The filtrate was reduced in volume, loaded onto a short alumina column, and then eluted with mixed solvents of THF (or ethyl acetate)–hexane. The solvents were removed *in vacuo* to yield (pale) yellow powers. Pure products were obtained either by layering concentrated CH$_2$Cl$_2$ solution with hexane, or by diethyl ether vapour diffusion into the concentrated CH$_2$Cl$_2$ solutions.

[(PPh$_3$)Au(C≡C–(C$_4$H$_2$S)(C$_4$H$_3$S))] 1. Synthesis was by the general procedure using the freshly prepared alkyne obtained from 40 mg (0.15 mmol) 5-(trimethylsilylethynyl)-2,2′-bithiophene (**TMSL^1**) and 76 mg (0.15 mmol) [Au(PPh$_3$)Cl]. Yield: 55 mg (55%), brownish crystals. IR (CH$_2$Cl$_2$): v(C≡C) 2104 cm^{-1} (vw). ^{1}H NMR (500 MHz, CDCl$_3$): δ 6.95 (d, $^3J_{HH}$ = 3.8 Hz, 1H, H^4), 6.97 (dd, $^3J_{HH}$ = 5.1 Hz, $^3J_{HH}$ = 3.6 Hz, 1H, H$^{4'}$), 7.04 (d, $^3J_{HH}$ = 3.8 Hz, 1H, H^3), 7.11 (dd, $^3J_{HH}$ = 3.6 Hz, $^4J_{HH}$ = 1.1 Hz, 1H, H$^{3'}$), 7.16 (dd, $^3J_{HH}$ = 5.1 Hz, $^4J_{HH}$ = 1.1 Hz, 1H, H$^{5'}$), 7.43–7.57 (m, 15H, H of PPh$_3$). ^{13}C NMR (500 MHz, CDCl$_3$): δ 96.03, 96.25 (–C≡C–); 123.20, 123.59, 124.19, 124.22 (ipso-C), 127.68, 131.99, 136.49 (ipso-C), 137.42 (ipso-C) (aromatic C of thiophenes); 129.08, 129.17, 129.38 (ipso-C), 129.83 (ipso-C), 131.55, 134.21, 134.32 (C of PPh$_3$). ^{31}P\{^{1}H\} NMR (400 MHz, CDCl$_3$): δ 42.78. LSIMS (m/z): 648 (calc. M_r = 648.529). Anal. calc. for AuC$_{28}$H$_{20}$PS$_2$: C, 51.86; H, 3.11. Found: C, 51.47; H, 3.10%.

[Au(PPh$_3$)(C≡C–(C$_4$H$_2$S)–C≡C)Au(PPh$_3$)] 2. Synthesis was by the general procedure using the freshly prepared alkyne obtained from 45 mg (0.16 mmol) 2,5-bis(trimethylsilylethynyl)thiophene [(TMS)$_2$L^2] and 150 mg (0.30 mmol) [Au(PPh$_3$)Cl]. Yield: 115 mg (67%), brownish crystals. IR (CHCl$_3$): v(C≡C) 2103 cm^{-1} (vw). ^{1}H NMR (500 MHz, CDCl$_3$): δ 6.94 (s, 2H, H of thiophene), 7.41–7.55 (m, 30H, H of PPh$_3$). ^{13}C NMR (500 MHz, CDCl$_3$): δ 96.40, 96.61 (–C≡C–); 124.50 (ipso-C), 130.82 (aromatic C of thiophenes); 129.05, 129.14, 129.44 (ipso-C), 129.88 (ipso-C), 131.50, 134.21, 134.32 (C of PPh$_3$). ^{31}P\{^{1}H\} NMR (400 MHz, CDCl$_3$): δ 42.78. LSIMS (m/z): 1048 (calc. M_r = 1048.682). Anal. calc. for Au$_2$C$_{44}$H$_{32}$P$_2$S: C, 50.40; H, 3.08. Found: C, 49.71; H, 3.09%.

[(PPh$_3$)Au(C≡C–(C$_4$H$_2$S)$_2$–C≡C)Au(PPh$_3$)] 3. Synthesis was by the general procedure using the freshly made alkyne obtained from 40 mg (0.11 mmol) 5,5′-bis(trimethylsilylethynyl)-2,2′-bithiophene [(TMS)$_2$L^3] and 110 mg (0.22 mmol) [Au(PPh$_3$)Cl]. Yield: 40 mg (32%), yellow crystalline solid. IR (CH$_2$Cl$_2$): v(C$\cdots$C) 2104 cm^{-1} (vw). ^{1}H NMR (500 MHz, CDCl$_3$): δ 6.91 (d, $^3J_{HH}$ = 3.8 Hz, 2H, H$^{4\ and\ 4'}$), 7.01 (d, $^3J_{HH}$ = 3.8 Hz, 2H, H$^{3\ and\ 3'}$), 7.42–7.56 (m, 30H, H of PPh$_3$). ^{13}C NMR (500 MHz, CDCl$_3$): δ 96.19, 96.39 (–C≡C–); 123.14, 124.03 (ipso-C), 132.03, 136.57 (ipso-C) (aromatic C of thiophenes); 129.08, 129.17, 129.37 (ipso-C), 129.82 (ipso-C), 131.54, 134.21, 134.32 (C of PPh$_3$). ^{31}P\{^{1}H\} NMR (400 MHz, CDCl$_3$): δ 42.46. LSIMS (m/z): 1130.4 (calc. M_r = 1130.802). Anal. calc. for Au$_2$C$_{48}$H$_{34}$P$_2$S$_2$: C, 50.98; H, 3.03. Found: C, 51.01; H, 3.20%.

[(PCy$_3$)Au(C≡C–(C$_4$H$_2$S)$_2$–C≡C–)Au(PCy$_3$)] 4. Synthesis was by the general procedure using a freshly prepared alkyne obtained from 40 mg (0.11 mmol) 5,5′-bis(trimethylsilylethynyl)-2,2′-bithiophene [(TMS)$_2$L^3] and 115 mg (0.22 mmol) [Au(PCy$_3$)Cl]. Yield: 50 mg (38%), orange needle crystals. IR (CH$_2$Cl$_2$): v(C≡C) 2098 cm^{-1} (vw). ^{1}H NMR (500 MHz,

Table 3 Details of the crystal data, data collection parameters, structure solution and refinement for complexes **1**–**5**[a]

Parameter	1	2	3	4	5
Formula	$C_{28}H_{20}AuPS_2$	$C_{44}H_{32}Au_2P_2S$	$C_{50}H_{38}Au_2Cl_4P_2S_2$	$C_{50}H_{74}Au_2Cl_4P_2S_2$	$C_{52}H_{36}Au_2P_2S_3$
Crystal size/mm	$0.12 \times 0.09 \times 0.09$	$0.12 \times 0.12 \times 0.04$	$0.14 \times 0.09 \times 0.09$	$0.09 \times 0.08 \times 0.07$	$0.14 \times 0.09 \times 0.01$
M	648.50	1048.63	1300.60	1336.89	1212.86
Crystal system	Triclinic	Triclinic	Triclinic	Monoclinic	Triclinic
Space group	$P\bar{1}$ (no. 2)	$P\bar{1}$ (no. 2)	$P\bar{1}$ (no. 2)	$P2_1/c$ (no. 14)	$P\bar{1}$ (no. 2)
a/Å	9.8914(3)	9.0569(18)	8.7120(10)	7.5320(10)	12.048(2)
b/Å	10.8261(5)	18.121(4)	10.0190(10)	17.242(2)	13.262(2)
c/Å	13.2729(5)	22.624(5)	14.0250(10)	20.675(2)	14.486(3)
α/°	67.079(2)	94.81(3)	92.110(10)	90.0	103.569(12)
β/°	80.617(2)	94.82(3)	101.210(10)	96.027(6)	99.567(9)
γ/°	64.618(2)	98.62(3)	96.500(10)	90.0	93.739(12)
U/Å^3	1182.73(8)	3640.5(13)	1190.9(2)	2670.2(5)	2205.5(7)
Z	2	4	1	2	2
T/K	180(2)	180(2)	180(2)	180(2)	180(2)
D_c/g cm^{-3}	1.821	1.913	1.813	1.663	1.826
μ/mm^{-1}	6.478	8.227	6.566	5.859	6.895
θ Range/°	1.67–27.49	3.70–27.52	2.05–27.55	2.96–25.03	2.05–25.09
Data collected	13 044	114 112	7803	12 089	17 835
Unique data, R_{int}	5350, 0.0618	16 681, 0.0956	5419, 0.0376	4686, 0.0323	7723, 0.080
Parameters	289	991	271	505	532
R_1 (observed data)	0.0388	0.0413	0.0310	0.0306	0.0544
wR_2 (all data)	0.1825	0.1176	0.0955	0.0635	0.1398

[a] Click here for full crystallographic data (CCDC 181057–181061).

CDCl$_3$): δ 1.18–2.04 (m, 66H, H of PCy$_3$), 6.87 (d, $^3J_{HH} = 3.8$ Hz, 2H, H$^{4 \text{ and } 4'}$), 6.97 (d, $^3J_{HH} = 3.8$ Hz, 2H, H$^{3 \text{ and } 3'}$). ^{13}C NMR (500 MHz, CDCl$_3$): δ 25.84, 27.04, 27.13, 30.68 (CH$_2$ of PCy$_3$); 33.17 (d, $J_{CP} = 111$ Hz, CH of PCy$_3$); 95.59, 95.79 (–C≡C–); 122.95, 124.37 (ipso-C), 131.73, 136.33 (ipso-C) (aromatic C of thiophenes). ^{31}P{^{1}H} NMR (400 MHz, CDCl$_3$): δ 56.92. LSIMS (m/z): 1167.4 (calc. $M_r = 1167.09$). Anal. calc. for Au$_2$C$_{48}$H$_{70}$P$_2$S$_2$: C, 49.40; H, 6.05. Found: C, 49.21; H, 5.89%.

[(PPh$_3$)Au(C≡C–(C$_4$H$_2$S)$_3$–C≡C)Au(PPh$_3$)] 5. Synthesis was by the general procedure using the freshly prepared alkyne obtained from 50 mg (0.11 mmol) 5,5″-bis(trimethylsilyl-ethynyl)-2,2′:5′,2″-terthiophene **[(TMS)$_2$L^4]** and 110 mg (0.22 mmol) [Au(PPh$_3$)Cl]. Yield: 50 mg (37%), orange needle crystals. IR (CH$_2$Cl$_2$): ν(C≡C) 2105 cm^{-1} (vw). ^{1}H NMR (500 MHz, CDCl$_3$): δ 6.94 (d, $^3J_{HH} = 3.8$ Hz, 2H, H$^{4' \text{ and } 4''}$), 6.99 (s, 2H, H$^{3 \text{ and } 4}$), 7.04 (d, $^3J_{HH} = 3.8$ Hz, 2H, H$^{3' \text{ and } 3''}$), 7.43–7.57 (m, 30H, H of PPh$_3$). ^{13}C NMR (500 MHz, CDCl$_3$): δ 96.08, 96.29 (–C≡C–); 123.15, 124.16, 124.30 (ipso-C), 132.10, 136.10 (ipso-C), 136.23 (ipso-C) (aromatic C of thiophenes); 129.08, 129.17, 129.38 (ipso-C), 129.83 (ipso-C), 131.56, 134.21, 134.32 (C of PPh$_3$). ^{31}P{^{1}H} NMR (400 MHz, CDCl$_3$): δ 42.78. LSIMS (m/z): 1213.2 (calc. $M_r = 1212.922$). Anal. calc. for Au$_2$C$_{52}$H$_{36}$P$_2$S$_3$: C, 51.49; H, 2.99. Found: C, 51.24; H, 3.08%.

X-Ray crystallography

Suitable, single crystals of the complexes **1**–**5** were grown by slow evaporation from CH$_2$Cl$_2$ or CH$_2$Cl$_2$–hexane mixtures. These were mounted on glass fibres using a perfluoropolyether oil that freezes at reduced temperatures and holds the crystal static in the X-ray beam.[25] Data for each of the crystals were recorded on an Enraf Nonius Kappa CCD Diffractometer equipped with an Oxford Cryostream crystal cooling apparatus, and using graphite monochromated Mo-Kα radiation, $\lambda = 0.71069$ Å. A SORTAV absorption correction was applied to each data set. Details of the crystal data, data collection, and structure solution and refinement are listed in Table 3. The structures were solved by direct methods (SHELXS-86[26]) and by subsequent Fourier difference syntheses, and refined by full-matrix, least squares based on F^2 (SHELXL-97[27]). Hydrogen atoms were placed in idealised positions and allowed to ride on the relevant carbon atom, and refined with common isotropic displacement parameters. In the structure of **2** the

phenyl rings were positionally disordered over two sites, and the two sets of positions were refined with partial occupancy, summing to unity. Similarly, in **4** all the cyclohexyl rings and one of the thiophene rings were disordered, and these were modelled using two positions for each group. Both **3** and **4** had disordered dichloromethane solvent molecules in the lattice, and again the two positions of the groups were refined with partial occupancy. For each structure, in the final cycles of refinement a weighting scheme of the form $w = 1/[\sigma^2(F_o)^2 + (xP)^2 + yP]$, where $P = (F_o^2 + 2F_c^2)/3$ was introduced which resulted in a relatively flat analysis of variance. Refinement continued until convergence was reached.

References

1 S. J. Shieh, X. Hong, S. M. Peng and C. M. Che, *J. Chem. Soc., Dalton Trans.*, 1994, 3067; B. C. Tzeng, W. C. Lo, C. M. Che and S. M. Peng, *Chem. Commun.*, 1996, 181.
2 R. J. Puddephatt, *Chem. Commun.*, 1998, 1055.
3 V.-W. W. Yam and K. K.-W. Lo, *Chem. Soc. Rev.*, 1999, **28**, 323; V. W.-W. Yam, K. K.-W. Lo and K. M.-C. Wong, *J. Organomet. Chem.*, 1999, **578**, 3; W.-Y. Wong, K.-H. Choi, G. L. Lu, J. X. Shi, P. Y. Lai, S. M. Chan and Z. Lin, *Organometallics*, 2001, **20**, 5446.
4 I. R. Whittall, M. G. Humphrey, S. Houbrechts and A. Persoons, *Organometallics*, 1996, **15**, 5738; I. R. Whitall, M. G. Humphrey, M. Samoc and B. Luther-Davies, *Angew. Chem., Int. Ed. Engl.*, 1997, **36**, 370; S. Houbrechts, C. Boutton, K. Clays, A. Persoons, I. R. Whittall, R. H. Naulty, M. P. Cifuentes and M. G. Humphrey,

J. Nonlinear Opt. Phys. Mater., 1998, **7**, 113; A. M. McDonagh, N. T. Lucas, M. P. Cifuentes, M. G. Humphrey, S. Houbrechts and A. Persoons, *J. Organomet. Chem.*, 2000, **605**, 193.

5   D. Li, X. Hong, C. M. Che, W. C. Lo and S. M. Peng, *J. Chem. Soc., Dalton Trans.*, 1993, 2929.

6   V.-W. W. Yam and S. W. K. Choi, *J. Chem. Soc., Dalton Trans.*, 1996, 4227.

7   V.-W. W. Yam, S. W. K. Choi and K. K. Cheung, *Organometallics*, 1996, **15**, 1734.

8   M. J. Irwin, J. J. Vittal and R. J. Puddephatt, *Organometallics*, 1997, **16**, 3541.

9   M. A. MacDonald, R. J. Puddephatt and G. P. A. Yap, *Organometallics*, 2000, **19**, 2194.

10 W. J. Hunks, M. A. MacDonald, M. C. Jennings and R. J. Puddephatt, *Organometallics*, 2000, **19**, 5063.

11 D. Beljonne, H. F. Wittmann, A. Köhler, S. Graham, M. Younus, J. Lewis, P. R. Raithby, M. S. Khan, R. H. Friend and J. L. Brédas, *J. Chem. Phys.*, 1996, **105**, 3868; M. Younus, A. Köhler, S. Cron, N. Chawdhury, M. R. A. Al-Mandhary, M. S. Khan, J. Lewis, N. J. Long, R. H. Friend and P. R. Raithby, *Angew. Chem., Int. Ed.*, 1998, **37**, 3036; M. Younus, N. J. Long, P. R. Raithby and J. Lewis, *J. Organomet. Chem.*, 1998, **570**, 55; J. Lewis and P. R. Raithby, *J. Organomet. Chem.*, 1998, **556**, 219; C. J. Adams, S. L. James, X. Liu, P. R. Raithby and L. J. Yellowlees, *J. Chem. Soc., Dalton Trans.*, 2000, 63; J. S. Wilson, A. Köhler, R. H. Friend, M. K. Al-Suti, M. R. A. Al-Mandhary, M. S. Khan and P. R. Raithby, *J. Chem. Phys.*, 2000, **113**, 7627; J. S. Wilson, N. Chawdhury, M. R. A. Al-Mandhary, M. Younus, M. S. Khan, P. R. Raithby, A. Köhler and R. H. Friend, *J. Am. Chem. Soc*, 2001, **123**, 9412; H. Zhang, A. W. M. Lee, W.-Y. Wong and M. S. M. Yuen, *J. Chem. Soc., Dalton Trans.*, 2000, 3675; W.-Y. Wong, K.-H. Choi, G.-L. Lu and J.-X. Shi, *Macromol. Rapid Commun.*, 2001, **22**, 461; W.-Y. Wong, S. M. Chan, K.-H. Choi, K. W. Cheah and W. K. Chan, *Macromol. Rapid Commun.*, 2000, **21**, 453.

12 J. Lewis, N. J. Long, P. R. Raithby, G. P. Shields, W.-Y. Wong and M. Younus, *J. Chem. Soc., Dalton Trans.*, 1997, 4283.

13 N. Chawdhury, A. Köhler, R. H. Friend, W.-Y. Wong, J. Lewis, M. Younus, P. R. Raithby, T. C. Corcoran, M. R. A. Al-Mandhary and M. S. Khan, *J. Chem. Phys.*, 1999, **110**, 4963.

14 P. Bäuerle, F. Wüother, G. Götz and F. Effenberger, *Synthesis*, 1993, 1099.

15 S. Takahashi, Y. Kuroyama, K. Sonogashira and N. Hagihara, *Synthesis*, 1980, 627.

16 R. H. Naulty, M. P. Cifuentes, M. G. Humphrey, S. Houbrechts, C. Boutton, A. Persoons, G. A. Heath, D. C. R. Hockless, B. Luther-Davies and M. Samoc, *J. Chem. Soc., Dalton Trans.*, 1997, 4167; I. R. Whittall, M. G. Humphrey, M. Samoc, B. Luther-Davies and D. C. R. Hockless, *J. Organomet. Chem.*, 1997, **544**, 189; I. R. Whittall, M. G. Humphrey, S. Houbrechts, J. Maes, A. Persoons, S. Schmid and D. C. R. Hockless, *J. Organomet. Chem.*, 1997, **544**, 277.

17 N. C. Baenziger, W. E. Bennett and D. M. Soboroff, *Acta Crystallogr., Sect. B*, 1976, **32**, 962.

18 P. Pyykkö, J. Li and N. Runeberg, *Chem. Phys. Lett.*, 1994, **218**, 233.

19 H. Schmidbaur, W. Graf and G. Müller, *Angew. Chem., Int. Ed. Engl.*, 1988, **27**, 417.

20 M. I. Bruce and D. N. Duffy, *Aust. J. Chem.*, 1986, **39**, 1697.

21 J. B. Birks, *Photophysics of Aromatic Molecules*, Wiley-Interscience, London, 1970.

22 W. L. F. Armarego and D. D. Perrin, *Purification of Laboratory Chemicals*, Butterworth Heinemann, Bath, UK, 4th edn., 1996.

23 M. I. Bruce, B. K. Nicholson and O. Bin Shawkataly, *Inorg. Synth.*, H. D. Kaesz, ed., 1989, **26**, 325.

24 R. Uson, A. Laguna and M. Laguna, *Inorg. Synth.*, H. D. Kaesz, ed., 1989, **26**, 86.

25 D. Stalke and T. Kottke, *J. Appl. Crystallogr.*, 1993, **26**, 615.

26 G. M. Sheldrick, SHELXS-86, Program for Crystal Structure Solution, University of Göttingen, Germany, 1986.

27 G. M. Sheldrick, SHELXL-97, Program for Crystal Structure Refinement, University of Göttingen, Germany, 1997.